

Structural Control and Properties of Low-Dielectric-Constant Poly(hydrogen silsesquioxane) Precursors and Their Thin Films

Wei-Chih Liu,¹ Yang-Yen Yu,¹ Wen-Chang Chen^{1,2}

¹Department of Chemical Engineering, National Taiwan University, Taipei, Taiwan 10617

²Institute of Polymer Science and Engineering, National Taiwan University, Taipei, Taiwan 10617

Received 3 April 2003; accepted 25 July 2003

ABSTRACT: The precursors of poly(hydrogen silsesquioxane) (PHSSQ) were synthesized from triethoxysilane (TES) through variations in the pH and molar ratio of water to TES (R_1). The molecular structures of the prepared PHSSQ precursors were controlled by the reaction conditions, including the molecular weight, the content of Si—OH end groups, and the cage/network ratio. The effect of the reaction conditions on the PHSSQ structure was quite different from that previously reported for poly(methyl silsesquioxane) (PMSSQ). The Si—OH content and cage/network ratio of the prepared PHSSQ precursors increased with increasing R_1 and pH. The molecular weight of the prepared PHSSQ precursors first increased with increasing R_1 or pH and then decreased at high values of R_1 . These results were

explained by the effects of R_1 and pH on the hydrolysis and condensation reactions. The cage/network ratio of the prepared PHSSQ films decreased with increasing curing temperatures and resulted in an increasing refractive index or dielectric constant. The steric effect from the side groups yielded PMSSQ films that had a smaller refractive index or dielectric constant than the PHSSQ precursors. PHSSQ films have potential applications as low-dielectric-constant materials. © 2003 Wiley Periodicals, Inc. *J Appl Polym Sci* 91: 2653–2660, 2004

Key words: dielectric properties; films; polysiloxanes; refractive index

INTRODUCTION

Poly(silsesquioxane)s, with a formula of $(\text{RSiO}_{3/2})_n$, have been extensively studied because of their outstanding thermal, chemical, mechanical, and electronic properties.¹ R can represent hydrogen, alkyl, aryl, or other organic groups with functional derivatives. Applications of silsesquioxane-related materials as new kinds of engineering plastics, dielectric materials, additives, and preceramics have been demonstrated recently.^{2–5}

Poly(hydrogen silsesquioxane) (PHSSQ) and poly(methyl silsesquioxane) (PMSSQ) have been recognized as low-dielectric-constant materials for deep submicrometer integrated-circuit processes.^{6–11} The chemical structures of PHSSQ and PMSSQ contain both Si—O—Si cages and network structures. The physical properties of PHSSQ and PMSSQ, such as the refractive index and dielectric constant, can be varied through the ratio of the cage to the network structure by thermal curing. The Si—OH content of PHSSQ and PMSSQ was important

for the crosslinking density of the prepared films. Recently, it has been proved that the Si—OH content can control the nanopore structure through a nanocomposite of PMSSQ/poly(methyl methacrylate-co-dimethylaminoethyl methacrylate (P(MMA-co-DMAEMA))).¹² Hence, controlling the molecular structures of poly(silsesquioxane)s is very important for their applications.

The synthesis and structural control of PMSSQ through the formulation and reaction conditions have been reported in the literature.^{11d,13,14} We have developed a method for controlling the molecular structure of PMSSQ, including the molecular weight, the Si—OR end-group content, and the cage/network ratio, through the variation of the ratio of the water to the monomer and the pH value.^{11d} The cage/network transformation and physical properties of the prepared PMSSQ films can also be monitored through thermal curing. However, the synthesis and structural control of PHSSQ have not been fully explored yet. Frye and Collins¹⁵ successfully prepared hydrogen silsesquioxane (HSSQ) from trichlorosilane with sulfuric acid. However, the prepared HSSQ had no Si—OH end groups, and so further hybridization with other materials through the end group was not possible. Sakamoto and Hagiwara¹⁶ replaced the sulfuric acid catalyst with nitric acid and obtained PHSSQ with Si—OH end groups. However, precise control over the molecular structure of PHSSQ, including the

Correspondence to: W.-C. Chen (chenwc@ntu.edu.tw).

Contract grant sponsor: National Science Council of Taiwan; contract grant numbers: NSC90-2216-E002-015 and ND-L-91S-C-057.

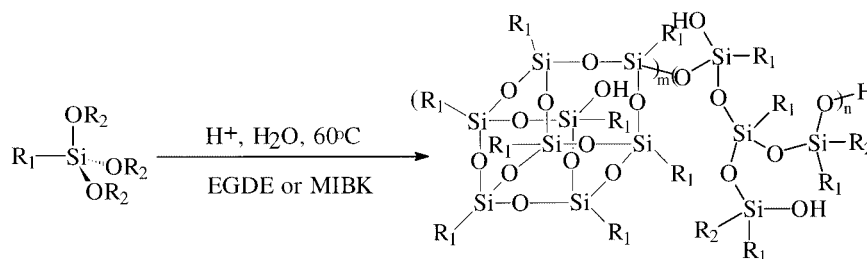


Figure 1 Synthetic scheme for the preparation of poly(silsesquioxane) precursors (PHSSQ, $R_1 = \text{H}$ and $R_2 = \text{C}_2\text{H}_5$; PMSSQ, $R_1 = \text{CH}_3$ and $R_2 = \text{CH}_3$).

molecular weight, Si—OH end-group content, and cage/network ratio, has not been achieved. Besides, it should be interesting to compare the molecular structures and properties of PHSSQ and PMSSQ precursors and their thin films.

In this study, the synthesis and structural control of PHSSQ precursors were systematically investigated through variations in the pH and molar ratio of H_2O to triethoxysilane (TES; R_1). The reaction scheme is shown in Figure 1. The PHSSQ precursors were spin-coated and cured to obtain low-dielectric-constant films. The content of the functional end groups (Si—OH), the molecular weight, and the cage/network ratio of the PHSSQ precursors were correlated with the pH and R_1 . The molecular structures of the synthesized PHSSQ precursors were characterized and compared with those of the PMSSQ precursors. A cage-structure HSSQ crystal was prepared to compare the molecular structure of PHSSQ. The properties of the prepared PHSSQ thin films from their precursors were reported, including the surface planarity, refractive index, and dielectric constant. The refractive index and dielectric constant of the prepared PHSSQ and previously reported PMSSQ thin films were correlated with their molecular structures.

EXPERIMENTAL

Materials

TES (95%; Aldrich, Milwaukee, WI), ethylene glycol dimethyl ether (EGDE; 99.7%; Tedia, Fairfield, OH), hydrochloric acid (35%; Yakuri, Osaka, Japan), nitric acid (69.9%; Tedia), and acetone- d_6 (99.9%; CIL, Lawrence, MA) were used as received. PMSSQ [weight-average molecular weight (M_w) = 7000–8000, average OH content = 5%; Gelest, PA] was used as a reference when we obtained the approximate content of Si—OH in the synthesized precursors.

Preparation of the PHSSQ thin films

The synthetic approach for preparing the PHSSQ precursors was similar to that for preparing the PMSSQ

precursors in the previous report.^{11d} However, the reaction medium in this study was EGDE, which was different from the previously used methyl isobutyl ketone (MIBK). The reaction conditions were varied with the molar ratio of the water to the monomer (R_1) and the pH value. The details of the preparation can be described with the following example. With the reaction conditions $R_1 = 1.5$ and $\text{pH} = 1.0$, 3.70 g of TES and 5.25 g of EGDE were added to a three-necked, 100-mL, round-bottom flask, which was immersed in an ice bath. Deionized water (0.58 g) with 0.15 g of HNO_3 in 5.0 g of EGDE was added dropwise over a period of 30 min with rigorous stirring. The reaction flask was allowed to warm to room temperature. It was then immersed in silicon oil at 60°C . The hydrolysis and condensation reaction were run for 3 h under a nitrogen atmosphere with reflux. The precursor solution of PHSSQ was then obtained. R_1 was set at 1.5, 2.0, 2.5, or 3.0 so that we could obtain various molecular structures of PHSSQ precursors, whereas the pH was adjusted to 1.0, 2.0, 3.0, or 4.0.

For the preparation of the films, PHSSQ precursors were spin-coated onto a silicon wafer at 3000 rpm for 20 s with a spin coater (PM490, Swien Co., Taiwan) at room temperature. The film was then baked at 80, 150, and 200°C on a hot plate for 10 min and cured at 400°C in a furnace under a nitrogen flow for 30 min.

Preparation of cage HSSQ

The single crystal of HSSQ cage was prepared with the literature method by Agaskar,¹⁷ which was used as a reference to confirm the existence of the cage structure in the prepared PHSSQ precursors and films. The structure of the prepared HSSQ crystal was analyzed by $^1\text{H-NMR}$, Fourier transform infrared (FTIR), and single-crystal X-ray diffraction, and it was compared with that reported in the literature.^{15,17,18}

Characterization

$^1\text{H-NMR}$ spectra of the prepared PHSSQ precursors were obtained with a JEOL (Tokyo, Japan) Ex-400

NMR spectrometer at 399.65 MHz. Acetone- d_6 was used as the deuterated solvent for the NMR measurements. The molecular weight of the prepared PHSSQ precursors was determined by gel permeation chromatography (GPC). The GPC system consisted of an elution column (PLgel 5- μm mixed C and D, Polymer Laboratories, Amherst, MA) and a refractive-index detector (RI2000, Badhonnf, Germany; Schambeck SFD GmbH). It was operated at 40°C with tetrahydrofuran as an eluent at 1 mL/min.

FTIR spectra of the synthesized PHSSQ precursors and corresponding thin films, prepared on double-polished silicon wafers, were obtained with a Jasco (Tokyo, Japan) FT/IR-410 spectrometer. The ratio of the Si—O—Si cage structure to the Si—O—Si network structure of the prepared PHSSQ precursors and films was obtained by a comparison of the peak areas of the 1127- and 1070- cm^{-1} peaks with an integral function. The Si—OH content in the PHSSQ precursors was determined as follows. The integral function of the FTIR spectra was performed to calculate the peak areas at 1300–1000 and 930–900 cm^{-1} , which were assigned to the Si—O—Si and Si—OH groups, respectively. By a comparison with a reference PMSSQ sample from Gelest with a reported OH content of 5%, the approximate content of Si—OH in the synthesized PHSSQ precursors was estimated. Although this is not an accurate method for determining the Si—OH content in the prepared precursors, it still provides information on the effect of the reaction conditions on the Si—OH content in the precursors.

The prepared crystal of HSSQ was analyzed with a single-crystal X-ray diffractometer (CAD4 Kappa Axis, Nonious (XRD) (Delft, The Netherlands). The crystal was radiated with Mo $K\alpha$ ($\lambda = 1.54056 \text{ \AA}$), and the data collection range was 3.70–27.44°. The bond angles, bond lengths, and Oak Ridge thermal ellipsoid plots (ORTEP) were obtained.

The properties of the prepared poly(silsesquioxane) films were characterized as follows. A prism coupler (model 2010, Metricon Co., Pennington, NJ) and an n & k analyzer (model 1200, n & k Technology, Inc., Santa Clara, CA) were used to measure the refractive index at 632.8 nm and the thickness of the prepared films. An atomic force microscope (DI5000 AFM, Digital Instrument, Inc., Woodbury, NY) was used to probe the surface morphology. The dielectric constant of the coated film was determined with a metal (Al)–insulator–semiconductor (MIS) device. In this measurement, the capacitance of the MIS device was measured with a Keithley model 82 C–V system (Cleveland, OH). The dielectric constant (k) was then calculated with the following formula: $k = ct/A\epsilon_0$, where c , t , A , and ϵ_0 are the observed capacitance, the film thickness, the area in contact with the measured film, and the free permittivity, respectively.

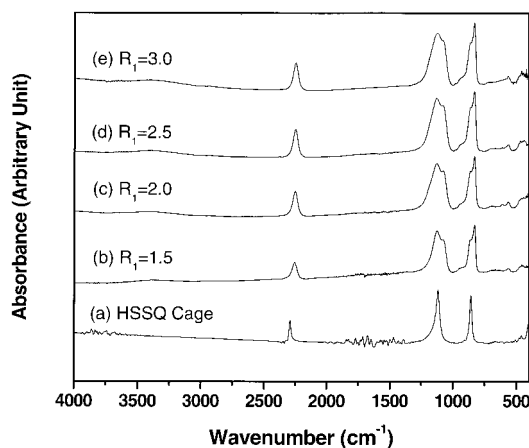


Figure 2 FTIR spectra of (a) the prepared HSSQ cage and (b–e) the PHSSQ precursors (pH 4, $R_1 = 1.5\text{--}3.0$).

RESULTS AND DISCUSSION

Figure 2(a) shows the FTIR spectrum of the prepared cage HSSQ. There are three major bands at 858, 1117, and 2292 cm^{-1} for the prepared cage HSSQ, which are assigned to the absorption bands of Si—H rocking, Si—O—Si stretching, and Si—H stretching, respectively. The positions of the three observed bands are similar to those reported in the literature.^{15,19} The chemical shift of Si—H for the prepared cage HSSQ in $^1\text{H-NMR}$ (benzene- d_6) is 4.21, which is the same as that reported by Agaskar.¹⁷ The chemical shifts of Si—H and Si—OH are similar to those reported in the literature.^{17,20} The ORTEP results for the single-crystal X-ray diffraction analysis showed that the prepared HSSQ crystal had the T_8 cage structure. The bond angle of Si—O—Si and the bond length of Si—O are 148.33–148.52° and 1.609–1.613 \AA , respectively, which are similar to those reported in the literature.¹⁸ These results confirm that the cage HSSQ was prepared successfully.

Figure 2(b–e) shows the FTIR spectra of the prepared PHSSQ precursors at pH 4.0 for various R_1 values. The Si—O—Si, Si—OH, and Si—H absorption bands of the prepared PHSSQ precursors are shown at 1300–1000, 930–900, and 2252 and 800–900 cm^{-1} , respectively. The Si—O—Si band of the prepared PHSSQ precursors splits into two bands at 1127 and 1070 cm^{-1} . The peak position of the Si—O—Si band at 1127 cm^{-1} in Figure 2(b–e), similar to that in Figure 2(a), suggests the existence of the Si—O—Si cage structure in the prepared PHSSQ precursors. The 1070- cm^{-1} band in the spectra of Figure 2(b–e) can be assigned to the Si—O—Si network absorption band. The peak positions of the Si—O—Si cage and network absorption bands are similar to those reported in the literature.^{6–8,11,12} It is not completely accurate to assign the splitting Si—O—Si bands to the cage and network structure because of the overlapping of the

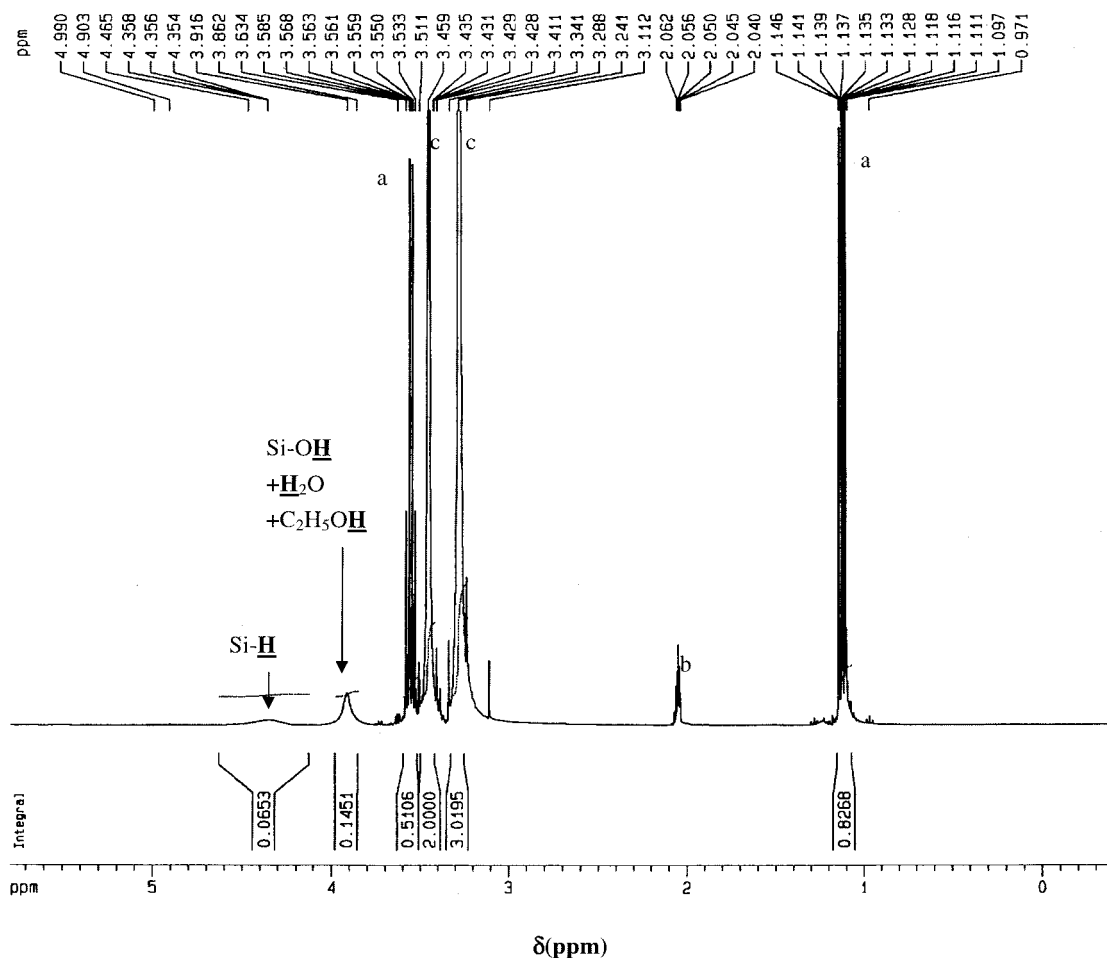


Figure 3 $^1\text{H-NMR}$ plot of the prepared PHSSQ precursor ($R_1 = 1.5$, pH 4): (a) $\text{C}_2\text{H}_5\text{OH}$, (b) acetone- d_6 , and (c) EGDE.

absorption bands. However, it can be used as a guideline to estimate the cage/network structural transformation.^{6-8,11,12}

Figure 3 shows the $^1\text{H-NMR}$ spectra of the PHSSQ precursors synthesized at $R_1 = 1.5$ and pH 4.0. The symbols a, b, and c in the $^1\text{H-NMR}$ spectra are assigned to the reaction side products and solvents: $\text{C}_2\text{H}_5\text{OH}$, acetone- d_6 , and EGDE, respectively. The chemical shifts of Si-H and Si-OH can be observed at 4.36 and 3.92 ppm, respectively. The Si- OC_2H_5 peak cannot be observed at the chemical shift of 3.80 ppm, and this suggests the complete hydrolysis of TES. Because the chemical shift of the Si-OH peak is complicated by $\text{C}_2\text{H}_5\text{OH}$ and H_2O , it is difficult to obtain the accurate Si-OH content only from the $^1\text{H-NMR}$ spectrum. An estimation of the Si-OH content of the PHSSQ precursors from the FTIR spectra is discussed later.

Figure 4 shows the effects of pH and R_1 on the Si-OH content of the prepared PHSSQ precursors in comparison with the previously reported PMSSQ precursors.^{11d} The Si-OH content was estimated from a comparison of the FTIR spectra of the synthe-

sized PHSSQ precursors with that of commercially available PMSSQ with an Si-OH content of 5%. The content of the Si-OH end groups in the prepared

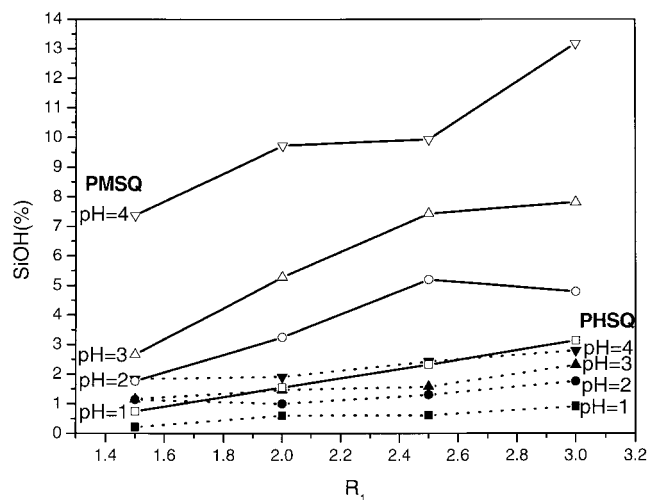


Figure 4 Effects of pH and R_1 on the Si-OH content of the prepared (—) PHSSQ and (---) PMSSQ precursors.

TABLE I
Molecular Structures and Properties of the Prepared PHSSQ Precursors and Their Corresponding Films

Reaction condition		PHSSQ precursor					PHSSQ film					
R_1	pH	Si—OH (%)	Cage/network	M_n	M_w	PDI	h (Å)	R_g (Å)	R_q (Å)	Cage/network	n	ϵ
1.5	1.0	0.21	2.01	2763	9,658	3.50	1974	2.61	3.39	0.95	1.405	2.87
	2.0	1.14	1.97	2083	5,496	2.64	1793	2.47	3.28	0.91	1.402	2.84
	3.0	1.16	2.12	2011	5,334	2.66	1717	2.39	3.37	0.97	1.399	2.78
	4.0	1.84	2.43	1872	4,687	2.50	1761	2.56	3.25	0.97	1.399	2.89
2.0	1.0	0.60	2.20	4354	21,518	4.94	1939	2.33	3.30	0.89	1.398	2.94
	2.0	1.00	2.19	3245	12,425	3.83	1715	2.24	2.95	0.93	1.403	2.82
	3.0	1.47	2.31	2874	11,985	4.17	1668	2.23	3.16	0.84	1.404	2.90
	4.0	1.91	2.54	2939	10,657	3.63	1701	2.29	3.20	0.89	1.403	2.88
2.5	1.0	0.61	2.33	4205	25,395	6.04	2257	2.99	3.96	0.95	1.391	2.74
	2.0	1.30	2.35	3057	12,577	4.11	1746	2.30	3.21	0.85	1.402	3.01
	3.0	1.58	2.42	2846	10,942	3.84	1609	2.30	3.15	0.82	1.405	2.98
	4.0	2.43	2.76	2895	11,141	3.85	1693	2.35	3.49	0.93	1.403	2.92
3.0	1.0	0.91	2.38	3043	16,292	5.35	2072	2.42	3.41	0.94	1.396	2.75
	2.0	1.76	2.37	2703	8,730	3.23	1615	2.30	3.20	0.92	1.400	2.91
	3.0	2.30	2.49	2287	8,007	3.50	1722	2.25	3.17	0.95	1.404	2.85
	4.0	2.79	2.96	2554	8,117	3.18	1606	2.23	3.04	0.84	1.405	2.96

h = film thickness; n = refractive index; ϵ = dielectric constant.

PHSSQ precursors are listed in Table I. The estimated Si—OH content shown in Figure 4 increases with increasing R_1 from 1.5 to 3.0. As R_1 increases, it enhances the hydrolysis reaction of the Si—OC₂H₅ group of the monomer TES. Thus, most of the Si—OC₂H₅ is hydrolyzed to become Si—OH, and this is also suggested by the ¹H-NMR results. This explains the trend of the Si—OH content of the prepared PHSSQ precursors with R_1 shown in Figure 4. Another trend observed from Figure 4 is that the Si—OH content of the prepared PHSSQ precursors decreases as the pH decreases. It has been reported in the literature²¹ that the acid-catalyzed condensation mechanism involves a protonated silanol species. Hence, the low-pH condition promotes the condensation reaction of the Si—OH group or the Si—OC₂H₅ group and thus reduces the Si—OH content. Therefore, the smaller Si—OH content of the prepared PHSSQ precursor is observed at lower pH values. As shown in Figure 4, the Si—OH content of the prepared PHSSQ precursors is lower than that of PMSSQ at the same R_1 and pH values. The Si—H side group of the prepared PHSSQ precursors, smaller than the Si—CH₃ side group of the PMSSQ precursors, probably enhances the condensation reaction of the Si—OH or Si—OR group. Thus, a difference is observed between the Si—OH contents in the prepared PHSSQ and PMSSQ precursors.

The ratios of the Si—O—Si cage and network structure have been obtained from a comparison of the peak areas between 1300 and 1000 cm⁻¹ by the integral function, and they are listed in Table I. Figure 5 shows the variation of the cage/network ratio of the prepared PHSSQ precursors and the previously reported PMSSQ^{11d} with R_1 and pH. For the PHSSQ and

PMSSQ precursors, there is a trend toward increased cage/network ratios with increasing R_1 . However, the opposite trend is found for the effect of the pH on the cage/network ratio. The hydrolysis rate increases with increasing R_1 , and so most Si—OR in the monomer converts into Si—OH. The functional group of Si—OH in the vicinity is subjected to intramolecular condensation, and the cage structure is formed. The condensation rate between Si—OH increases with decreasing pH and forms the network structure. Thus, the cage/network ratio of the prepared PHSSQ precursors decreases with increasing pH. Because the PHSSQ precursors have smaller side groups than the

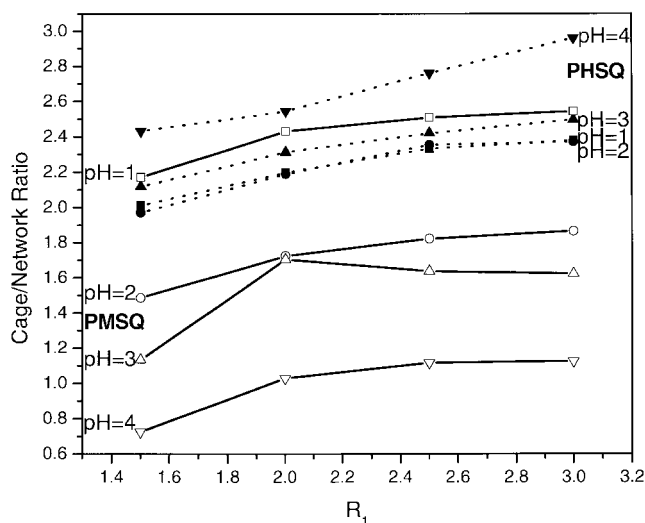


Figure 5 Effects of pH and R_1 on the cage/network ratio of the prepared (---) PHSSQ and (—) PMSSQ precursors.

PMSSQ precursors, the condensation to form the network structure by the intermolecular reaction is easier. Hence, the cage/network ratio of the PMSSQ precursors is higher than that of the PHSSQ precursors at pH 1. As the pH increases, the hydrolysis reaction of Si—OCH₃ to Si—OH is difficult for the PMSSQ precursors and thus retards the cyclization reaction of the PMSSQ precursors at a high pH. Therefore, the cage/network ratio increases with increasing pH for PMSSQ.

The molecular weight distribution, M_w , number-average molecular weight (M_n), and polydispersity index (PDI) of the prepared PHSSQ precursors from the GPC study are listed in Table I. The molecular weight first increases with increasing R_1 and then decreases. This can be explained as follows. For the condensation reaction in a sol-gel process, there are two reaction modes: water condensation and alcohol condensation. The rate of the former is faster than that of the latter. In water condensation, two silanol groups (hydrolysis with two water molecules) react and release one water molecule. That is, if there are n monomers initially, $3n$ mol of hydrolyzable alkoxy groups is completely hydrolyzed and condensed with $1.5n$ water molecules. This is the reason for the lowest R_1 value being set to 1.5. However, more than $1.5n$ of water molecules (i.e., $R_1 > 1.5$) might be necessary for completing the hydrolysis and condensation reaction because the nucleophile, water, would be disturbed in the reaction medium. Thus, the molecular weight increases with increasing R_1 . However, in the case of high R_1 values, excess water might result in the dissociation of the condensate siloxane bond and thus reduce the molecular weight. Hence, the trend of the molecular weight of the prepared PHSSQ precursor with R_1 is observed. Another trend shown in Table I is that the molecular weight of the prepared PHSSQ precursors increases with decreasing pH. This is because the condensation rate in the acid-catalyzed sol-gel process is proportional to the protonated silanol species. Thus, a higher molecular weight can be obtained at a lower pH value. M_w and M_n of the prepared PHSSQ precursors are in the range of 1872–4354 and 4687–21,518, respectively. These values are much higher than that of PMSSQ reported previously,^{11d} which has a molecular weight of 474–2076. In fact, the previously reported PMSSQ was suggested to be an oligomer. The steric effect from the side group produces the higher condensation reaction rate of PHSSQ, with respect to PMSSQ, and thus yields a higher molecular weight.

Figure 6 shows the FTIR spectra of the prepared HSSQ cage and the PHSSQ (pH = 4.0, $R_1 = 1.5$) film on a double-polished silicon wafer as spun and at various curing temperature of 80, 150, 200, and 400°C, respectively. Two distinct changes can be observed from a comparison of the FTIR spectra in Figure 6. The

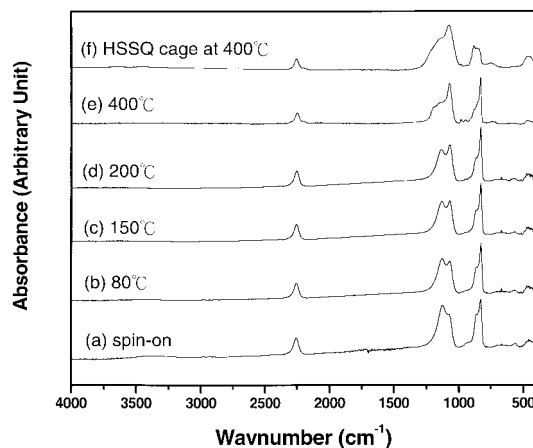


Figure 6 FTIR spectra of the prepared HSSQ cage at 400°C and the spun-on PHSSQ film ($R_1 = 1.5$, pH = 4) after curing at 80, 150, 200, or 400°C.

absorption peaks of the Si—OH groups at 3500 and 910 cm^{-1} of Figure 6(b) disappear at 400°C in Figure 6(e). This suggests that the condensation reaction of the Si—OH group takes place. Another distinct change is the peak intensity between 1000 and 1300 cm^{-1} . The intensity of the Si—O—Si absorption band of the cage structure at 1127 cm^{-1} decreases as the curing temperature increases. However, the Si—O—Si absorption band of the network structure at 1070 cm^{-1} shows the opposite trend. This indicates the transformation of the Si—O—Si cage structure to the network structure by thermal curing, just as reported in the literature.^{11a,11b} As shown in Table I, the cage/network ratio decreases from 1.97–2.96 for the PHSSQ precursors to 0.84–0.97 for the prepared films. The fully caged HSSQ also shows a similar cage/network structural transformation by thermal curing, as shown in Figure 6(f). Such a structural transformation is similar to that of PMSSQ reported previously.^{11d,22}

The electronic and optical properties of the prepared films, such as the refractive index and dielectric constant, are significantly affected by the cage/network structural transformation from thermal curing. Besides, the cage/network transformation significantly affects the thermal mechanical properties of the prepared PHSSQ. As suggested by Liou and Pretzer,⁷ the mechanical properties of the prepared PHSSQ increases as the cage/network ratio is reduced by thermal curing. Figure 7 shows the variation of the refractive index of the prepared PHSSQ films and the previously reported PMSSQ^{11d} with the cage/network ratio. The refractive index of the prepared PHSSQ and PMSSQ films decreases from 1.405 to 1.391 and from 1.396 to 1.363 as the cage/network ratio increases. For an insulating dielectric material, the refractive index is proportional to the ratio of the molar refraction to the molar volume.

Because the cage structure has a larger free volume than the network structure, this explains the trend of the refractive index with the cage/network ratio shown in Figure 7. The prepared PHSSQ film had a higher refractive index than PMSSQ at the same cage/network ratio, as shown in Figure 7. This is probably because PMSSQ with CH_3 groups results in steric hindrance between the polymer chain, and so PMSSQ has a higher free volume than PHSSQ. Figure 8 shows the variation of the dielectric constants of the prepared PHSSQ films and the previously reported PMSSQ^{11d} with the cage/network ratio. The trend for the dielectric constant with the cage/network ratio or the side group on the prepared poly(silsesquioxane) films is the same as that of the refractive index; this can be explained by the free-volume factor. The decreasing refractive index and dielectric constant as the cage/network ratio increases are consistent with our earlier study.²² The dielectric constants of the prepared PHSSQ films are 2.74–3.01, respectively, and the films may potential applications as low-dielectric-constant materials in deep submicrometer integrated circuit processes. The adjustable functional end group, refractive index, and film-forming properties have led to prepared poly(silsesquioxane) films being used as optical thin films.^{11e}

The film thickness (R_a) and surface roughness (R_q) of the prepared PHSSQ films are 1609–2257 and 2.25–3.96 Å, respectively, as shown in Table I. The ratio of R_q in comparison to the small R_a value, suggests excellent surface quality for the prepared PHSSQ films.

CONCLUSIONS

We have successfully synthesized structurally controllable PHSSQ from TES by varying the pH and R_1

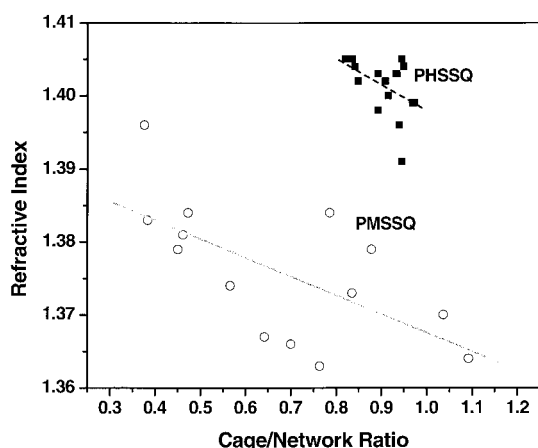


Figure 7 Variation of the cage/network ratio with the refractive index of the prepared (—) PHSSQ and (---) PMSSQ films after curing at 400°C for 30 min.

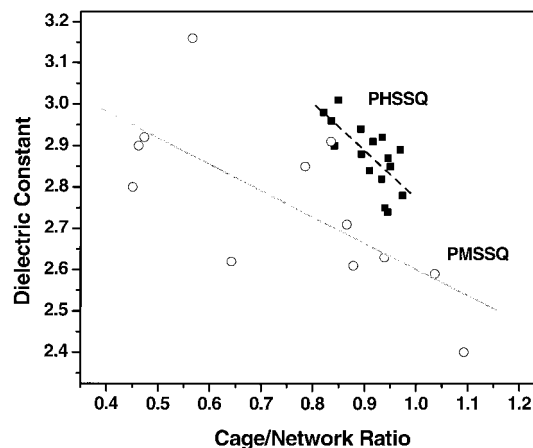


Figure 8 Variation of the cage/network ratio with the dielectric constants of the prepared (---)PHSSQ and (—) PMSSQ films after curing at 400°C for 30 min.

values. The Si—OH content and cage/network ratio of the prepared PHSSQ precursors increased with increasing R_1 and pH. The molecular weight of the prepared PHSSQ precursors first increased with increasing R_1 or pH and then decreased at high R_1 values. These results were explained by the effects of R_1 and pH on the hydrolysis and condensation reactions. The cage/network ratio of the prepared PHSSQ films decreased with increasing curing temperatures and resulted in the refractive index or dielectric constant increasing. The prepared poly(silsesquioxane)s have potential applications as low-dielectric-constant materials or optical films.

References

- Banley, R. H.; Itoh, M.; Sakakibara, A.; Suzuki, T. *Chem Rev* 1995, 95, 1409.
- Tamaki, R.; Tanaka, Y.; Asuncian, M. Z.; Choi, J.; Laine, R. M. *J Am Chem Soc* 2001, 123, 12416.
- Lichtenman, J. D.; Otonari, Y. A.; Carr, M. J. *Macromolecules* 1995, 28, 8435.
- Feher, F. J.; Rahimian, A.; Budzichowski, A.; Ziller, J. W. *Organometallics* 1995, 14, 3920.
- Siew, Y. K.; Sarkar, G.; Hu, X.; Hui, J.; See, A.; Chua, C. T. *J Electrochem Soc* 2000, 147, 201.
- Albrecht, M. G.; Blanchette, C. *J Electrochem Soc* 1998, 145, 4019.
- Liou, H. J.; Pretzer, J. *Thin Solid Films* 1998, 335, 186.
- Kohl, A. T.; Mimna, R.; Shick, R.; Rhodes, L.; Wang, Z. L. Kohl, P. A. *Electrochem Solid State Lett* 1999, 2, 77.
- Zhao, J. H.; Malik, I.; Ryan, T.; Ogawa, E. T.; Ho, P. S.; Shih, W. Y.; McKerrow, A. J.; Taylor, K. J. *Appl Phys Lett* 1999, 74, 944.
- Lee, H. J.; Lin, E. K.; Wang, H.; Wu, W. L.; Chen, W.; Moyer, E. S. *Chem Mater* 2002, 14, 1845.
- (a) Chen, W. C.; Lin, S. C.; Dai, B. T.; Tsai, M. S. *J Electrochem Soc* 1999, 146, 3004; (b) Chen, W. C.; Yen, C. T. *J Vac Sci Technol B* 2000, 18, 201; (c) Yang, C. C.; Chen, W. C. *J Mater Chem* 2002, 12, 1138; (d) Lee, L. H.; Chen, W. C.; Liu, W. C. *J Polym Sci Part A: Polym Chem* 2002, 40, 1560; (e) Chen, W. C.; Lee, L. H.; Chen, B. F.; Yen, C. T. *J Mater Chem* 2002, 12, 3644.

12. Huang, Q. R.; Volksen, W.; Huang, E.; Toney, M.; Frank, C. W.; Miller, R. D. *Chem Mater* 2002, 14, 3676.
13. Takamura, N.; Gunji, T.; Hatano, H.; Abe, Y. *J Polym Sci Part A: Polym Chem* 1999, 37, 1017.
14. Lee, J. K.; Char, K.; Rhee, H. W.; Ro, H. W.; Yoo, D. Y.; Yoon, D. Y. *Polymer* 2001, 42, 9085.
15. Frye, C. L.; Collins, W. T. *J Am Chem Soc* 1970, 92, 5586.
16. Sakamoto, Y. K.; Hagiwara, K. Y. U.S. Pat. 6,074,962 (2000).
17. Agaskar, P. A. *Inorg Chem* 1991, 30, 2707.
18. Earley, C. W. *J Phys Chem* 1994, 98, 8693.
19. Loboda, M. J.; Grove, C. M. Schneider, R. F. *J Electrochem Soc* 1998, 145, 2861.
20. *The Chemistry of Organic Silicon Compounds*; Patai, S.; Rapoport, Z., Eds.; Wiley: New York, 1989; Vol. 1, Part 2, p 512.
21. Brinker, C. J.; Scherer, G. W. *Sol-Gel Science: The Physics and Chemistry of Sol-Gel Processing*; Academic: Boston, 1990; Chapter 3.
22. Liu, W. C.; Yang, C. C.; Chen, W. C.; Dai, B. T.; Tsai, M. S. *J Non-Cryst Solids* 2002, 311, 233.